Geological and Vegetational Applications of Shuttle Imaging Radar-B, Mineral County, Nevada

M. X. Borengasser
Cooperative Institute for Aerospace Science and Terrestrial Applications, University of Nevada Reno, Reno, NV 89557
E. F. Kleiner
Department of Biology, University of Nevada Reno, Reno, NV 89557
P. Vreeland
Western Analytical Biogeographers, Inc., 1980 Carter Drive, Reno, NV 89509
F. F. Peterson
College of Agriculture, University of Nevada Reno, Reno, NV 89557
H. Klieforth
Atmospheric Sciences Center, Desert Research Institute, Reno, NV 89506
J. V. Taranik
Cooperative Institute for Aerospace Science and Terrestrial Applications, University of Nevada Reno, Reno, NV 89557

ABSTRACT: Multiple-incidence angle and multi-azimuth radar data were acquired from a Shuttle platform over test sites in Nevada in October 1984. An attempt was made to correlate these data with ground features for the purpose of evaluating the use of such data for geological and vegetational assessment. Standard ecological parameters with respect to the flora (community composition, dominance, and relative cover) were recorded in the field at the time of overflight. Although a total of 33 species representing 11 plant families were recognized, and plant cover ranged from 13 to 26 percent, radar data could not be used to separate plant communities. The signal return is more a function of abiotic conditions than vegetative characteristics. Illumination geometry plays an important role in the ability to detect strike-slip and dip-slip faults. Local incidence angle is the most important parameter, and SIR-B data takes with small incidence angles are superior for identifying certain styles of faulting. Look direction is critical for detecting faults with a dip-slip component. New structural features were not observed. Problems with radar antenna power and recording significantly affected data quality.

OBJECTIVES

THE OBJECTIVES of this investigation are to (1) determine the usefulness of spaceborne synethetic aperture radar (SAR) as a tool for large scale vegetation mapping, (2) to determine the optimum illumination geometry for spaceborne SAR, and (3) to refine existing tectonic models for the western Basin and Range Province.

The study area is located in the western Basin and Range Province of western Nevada. In this area there are a variety of desert plant communities, each with its own characteristic composition, cover, and relative tissue moisture. Soil types, and their associated water retention capacity, also vary within the study area. Because this is also the site of a SIR-B "crossover," where near-orthogonal ascending and descending SIR-B tracks coincide, it is an optimum site for the evaluation and utilization of SIR-B data for discrimination of desert plant communities.

The study area is also located within the Walker Lane structural zone, where both strike-slip and dip-slip faulting is common. Unlike typical Basin and Range faults, many of the faults within the study area are not range-front faults but may traverse both the ranges and the intermontane valleys. For these reasons, the study area is optimum for evaluating SIR-B illumination geometry for structural geology applications.

DESCRIPTION OF SIR-B DATA

Two sets of nearly orthogonal SIR-B data takes cross one another in the Candelaria region of western Nevada. One southwest to northeast track was also acquired over Death Valley, Yucca Mountain, and the Groom Range (Figure 1) at an incidence angle of 48°. For this investigation, three SIR-B data takes were used: Data Take AL87.4, Scene 5; Data Take AM82.2, Scene 4; and Data Take AM66.2, Scene 4 (Figure 1, Table 1). These three data takes were used because they provided good coverage of the study area and had relatively high signal-to-noise ratios.

SOIL MOISTURE STATUS OF STUDY AREA

Inasmuch as soil moisture affects radar penetration (Huete *et al.*, 1983; Brady, 1974), analyses of selected sites for soil types and for moisture at the time of the mission were conducted. Eight sites were chosen, three of which were studied intensively; the remainder were spot sampled. Gravimetric and volumetric moisture of soil profiles were sampled at 10-cm increments to a maximum depth of 70 cm. Auger samples were also used for gravimetric moisture determination. Sites were approximately 90 m^2 in size. Soil types included very sandy, extensive loamy, and gravelly sites as well as a very high clay content on the playa.

Soil moisture by weight in well-drained areas varied from 1 percent in upland sites to 5 percent in lowland sites, with 15 percent in the poorly-drained playa. All of the well-drained upland soils were dry with respect to plant growth during the mission. However, these soils did contain measurable amounts of water that were greatest in subsoil horizons and in soil materials with a greater clay content. This finding is consistent with the fact that the unavailable water for plants, i.e., that held at suctions greater than 15 bars, is held on and between the clay-sized particles (Brady, 1974). Inasmuch as soil moisture held in the upper few decimetres affected radar penetration, the effect should have been greatest for those soils with clay loam or clay subsoils and least for the sands and loamy sands. However, all upland soils were dry, so changes in radar signature did not reflect soil moisture differences.

VEGETATIONAL ANALYSIS

An attempt was made to evaluate SIR-B imagery as a tool for vegetational analysis. A field investigation was conducted 6–8

PHOTOGRAMMETRIC ENGINEERING AND REMOTE SENSING,
Vol. 54, No. 1, January 1988, pp. 71–76.

0099-1112/88/5401–71$02.25/0

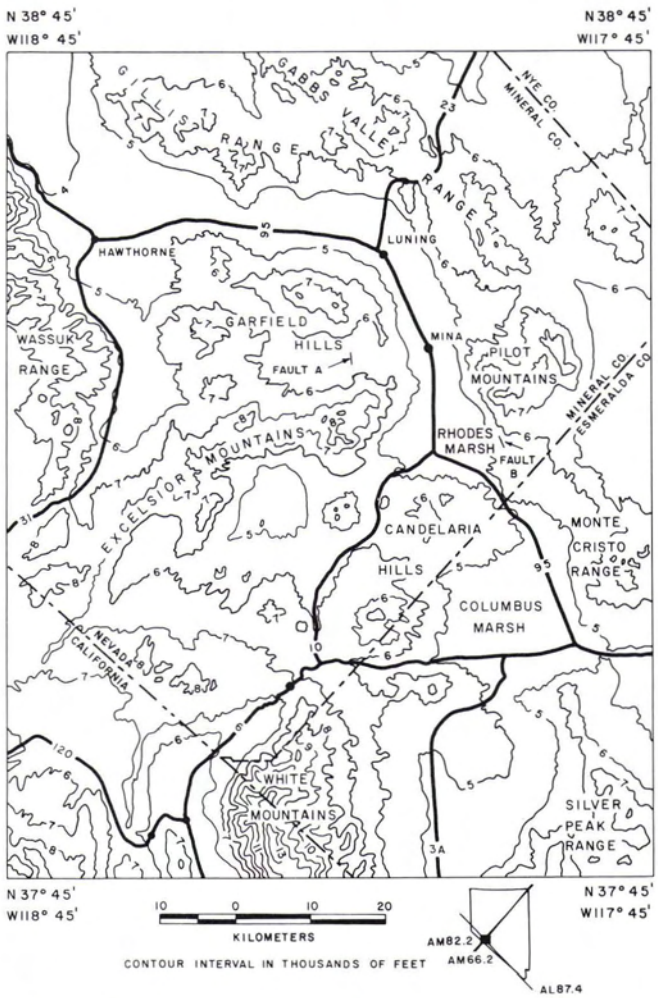

FIG. 1. General location map of SIR-B study area. Inset map shows location of SIR-B data takes used for this analysis.

October 1984. A variety of parameters was considered: (1) plant community composition, (2) density and dominance, (3) tissue moisture content, and (4) cover. Quantitative analyses were conducted where practical; otherwise a qualitative approach was taken.

SIR-B Data Take AL87.4 was utilized for vegetation analysis. In general, the study area around Hawthorne, Nevada falls within the shadscale vegetation zone of Nevada and eastern California as recognized by Billings (1949). More recently, this zone has been defined as the salt desert shrub zone of the desert shrub ecosystem (Fowler and Koch, 1982). In the higher elevations, the pinyon-juniper community can be found. All taxonomic references are in accordance with Munz (1959).

A total of 35 sites were studied, of which 29 were analyzed qualitatively. These 29 sites were considered only to give a broad overview of general species presence and approximate plant density. Sites were selected on the basis of distinctive visual differences in plant communities. Analysis consisted of a walk-through estimation of composition, presence, and relative dominance.

Quantitative analysis was conducted in two ways. The line intercept method was used at two sites to determine if differences in plant cover density could be detected from SIR-B data. Samples of root and shoot tissue were taken from woody and herbaceous species in six locations to determine the extent to which backscatter was affected by plant tissue moisture content. Three of the samples were in the pinyon-juniper upland and three were in the lower salt desert shrub communities. Moisture content was determined by weighing fresh tissue, drying for 48 hours at 120°C, then reweighing. A complete species presence list was prepared for the six sites.

Results of Vegetation Studies

A total of 33 species representing 11 plant families was recorded on the six sites. Two families, Asteraceae and Chenopodiaceae, account for 58 percent of the species present. If a third taxon, Poaceae, is included, 73 percent of the flora is encompassed.

Sixteen prevalent plant species from six sites were analyzed for total tissue (shoot plus root) moisture. Average percent moisture content ranges from a maximum of 62 percent in *Sphaeralcea ambigua*, a herbaceous perennial, to a minimum of 12 percent in a perennial grass, *Oryzopsis hymenoides*. In Table 2, the six sites sampled are arranged in diminishing order of total tissue moisture for all species present, ranging from a maximum of 58 percent in site 2a to a minimum of 24 percent in site 1. In Table 3, a comparison of vegetation cover is made between sites 1 and 2 for each species.

Botanical Applications of SIR-B Data

SIR-B imagery proved to be of little use for large scale vegetation mapping in the area around Hawthorne, Nevada. Differences in species distribution noted in the field were not discernible from the radar data. Several factors may have contributed to this lack of success.

(1) Canopy geometry and plant spacing affect radar signal return (Wardley *et al.*, 1987; Simonett, 1983). More than half of the species present represent two plant families. They share similar morphological characteristics with respect to leaf size and number, branching pattern, and overall size and configuration.

(2) Cross polarization (HV) has been found to enhance textural differences in naturally vegetated areas (Morain and Simonett, 1966). Like polarization (HH) of SIR-B data did not permit detection of subtle vegetation changes.

(3) Wavelengths approximately the size of the plant unit offer greatest potential for vegetation discrimination (Ulaby and Batlivala, 1976; Bush and Ulaby, 1978). L-band wavelength is smaller than the dominant components of the communities surveyed. Therefore, SIR-B data were not ideal for plant discrimination in this instance.

Although total plant cover varied from about 27 percent to 13 percent and tissue moisture from about 58 percent to 24 percent, these differences were not readily discernible from SIR-B data. Uneven soil surface features, considerable topographic variation at the study sites, similar gross morphology of shrub species, and relative sparseness of total plant cover made vegetational changes indistinguishable from ground return. Similar lack of success in extracting differential vegetation community information from radar imagery of semi-arid environments with cover less than 30 percent was reported by Heute *et al.* (1983).

Certain features, however, were discernible from SIR-B data. In one of the level study sites with a uniform plant community

TABLE 1. SUMMARY OF SIR-B DATA PARAMETERS.

Data Take	SNR	Center Inc.	Az Look Dir	$\Delta\Theta$ Across Swath	Swath Width	Resolution
AL87.4(5)	7.78dB	30.0°	215.2°	6.42°	27.2 km	28.2 m × 24.3 m
AM66.2(5)	6.33dB	39.9°	324.2°	4.11°	19.6 km	21.9 m × 25.6 m
AM82.2(5)	13.5dB	21.5°	323.2°	3.33°	15.5 km	38.3 m × 27.8 m

TABLE 2. HAWTHORNE SITES ARRANGED ACCORDING TO AVERAGE TOTAL TISSUE MOISTURE.

Site	Moisture ($\bar{x}$ %)
2a	58.2
2	44.5
Pepper Spring Summit	35.5
23	29.6
22	27.6
1	23.8

TABLE 3. AVERAGE COVER OF SPECIES BY SITE.

Species	Site 1 $\bar{x}$ % cover	Site 2 $\bar{x}$ % cover
Sarcobatus Baileyi	9.1	6.6
Menodora spinescens	5.6	
Salsola paulsonii	---	5.0
Artemisia spinescens	2.0	---
Atriplex confertifolia	1.2	1.1
Chrysothamnus nauseosus	0.1	---
Atriplex canescens	---	0.2
Sphaeralcea ambigua	---	0.2
Hilaria Jamesii	7.8	---
Oryzopsis hymenoides	0.9	0.1
Total % cover	26.7	13.2

composition and a smooth soil surface, an area with recent standing water appeared darker than nearby dryer locations. At another level site, areas with a cobbled surface texture appeared lighter than adjacent stabilized dunes. The sparse vegetation cover and similar species morphology permits L-band interaction with the soil surface; thus, the signal return appears to be indicative of abiotic rather than vegetative characteristics.

GEOLOGICAL ANALYSIS

For this analysis, several parameters related to radar illumination are used to describe the geometry between the incident radar signal and the landscape surface. The incidence angle is the angle between the incoming radar signal and the normal to the surface at the point of incidence; the nominal incidence angle of SIR-B data takes implies a horizontal surface at the point of incidence. Because few natural surfaces are horizontal, the local incidence angle is the angle between the radar signal and the normal to the local surface. Local incidence decreases on foreslopes and increases on backslopes by the amount of the local slope in each case.

CANDELARIA TEST SITE

The Candelaria test site, in southern Mineral County, includes the southern Excelsior Mountains, Rhodes Salt Marsh, and the northern Candelaria Hills (Figure 1). Between the two mountains is a large alluvial fan, sloping eastward towards Rhodes Salt Marsh. The southern margin of the Excelsior Range has been mapped as an east-trending fault zone, and is described as a normal fault by Dohrenwend (1982) and a right lateral strike slip fault by Stewart (1985). An explanation for the diverse trends of the Cenozoic rocks (Stewart, 1985) suggests that the Excelsior fault zone is continuous across the alluvial fan and through Rhodes Salt Marsh.

Data Takes AL87.4, AM82.2, and AM66.2 were computer enhanced to apply SIR-B data to the structural analysis of the Candelaria region. Computer enhancement was done with a VAX 11/780 IDIMS image processing system and involved contrast enhancement and filtering. Examination of the contrast-enhanced data revealed a lineament on Data Take AL82.2 in a location consistent with Stewart's (1985) tectonic model (Plate 1). No lineaments were detected on Data Takes AL87.4 (Plate 2) and AM66.2 (Plate 3). Because the look direction of AL87.4 is subparallel to the Excelsior fault zone, it was not expected to provide information about this structural feature and subsequent analysis was confined to AM82.2 and AM66.2.

A variety of linear and nonlinear contrast enhancements was employed to enhance the display of the proposed Excelsior fault zone. An exponential redistribution proved to be most satisfactory because of the ability to display subtle features within the alluvial fan and salt marsh. An alternate image product that was useful was produced by adding back 50 percent of a high-pass filtered image to the raw data. These two enhanced images, AM82.2 and AM66.2, and a Landsat TM false color composite (bands 5, 4, 3 = red, green, blue) were evaluated for detection of the proposed continuation of the Excelsior fault zone. These Landsat TM bands were optimum for displaying the geologic diversity of the area.

The lineament on the AM82.2 image is expressed as a diffuse, bright, relatively straight line within an area dominated by speckle (Plate 1). On the AM66.2 image, no lineament is visible, even after contrast enhancement and high-pass filtering (Plate 3). On the Landsat TM false color composite the suggested fault zone is expressed by a lineament that appears as a series of gullies from the Excelsior Mountains and Candelaria Hills (Plate 4). A tonal lineament was also observed, but was not coincident with the location of the proposed fault. Field examination revealed that the tonal lineament is the boundary of dark-colored hornblende andesite porphyry boulders from the Candelaria Hills and light-reddish granite boulders from the Excelsior Mountains. The lineament on the AM82.2 image (Plate 1) is caused by 8 to 9 subparallel gullies on the alluvial fan. The gullies are approximately 0.8 metres deep, 2.4 metres wide at the bottom, and 6.7 metres wide at the top. The bottoms of the gullies are predominately gravel, sand, and silt, in contrast to the boulders of the alluvial fan. Because AM66.2 has a greater angle of incidence, it would be expected to be more effective in delineating linear depressions such as the proposed continuation of the Excelsior fault zone.

In order to understand why AM82.2 is superior to AM66.2 for this application, and make recommendations for the optimum illumination geometry for structural geology, it is necessary to consider the configuration of the surface features with respect to the incident radar signal. Because more than 75 percent of the surface of the alluvial fan is covered with granite and andesite porphyry boulders ranging in size from 6.5 to 23 centimetres in the long dimension, the surface appears rough to L-band radar at both 21.5° and 40° incidence angles, and most features with a bright signature would be indiscernible. Additionally, the high degree of speckle will also tend to obliterate low-contrast surface features. Because the walls of the gullies slope from 19° to 21°, the 21.5° incidence angle of AM82.2 would result in a local incidence angle of from 2.5° to 0.5° on the sides of the gullies (Figure 2). The incidence angle of AM82.2 permits the incident radar signal to interact with the bottom of the gully with an angle of approximately 21.5° and, because the bottom of the gully is smooth to nearly-smooth to L-band, it would be a specular reflector and have a dark signature and a high contrast ratio with respect to the overall signature of the alluvial fan.

In much of Nevada, and throughout the Basin and Range Province, the geomorphic feature that marks the transition between the mountains and the basins is almost always an extensive alluvial fan. Although the characteristic structural style of the Basin and Range Province is normal faulting parallel to the range fronts, equally important styles of faulting are dip-slip and strike-slip faults that are transverse to intermontane valleys. Because faulting can control drainage and promote erosional processes, dip-slip and strike-slip faults parallel to drainage on alluvial fans can commonly be expressed as negative topographic features. Based on the above interpretation, imaging radar systems with small incidence angles appear to be more effective for delineating these types of faults within the western Basin and Range Province.

Although the SIR-B system acquired multi-incidence angle

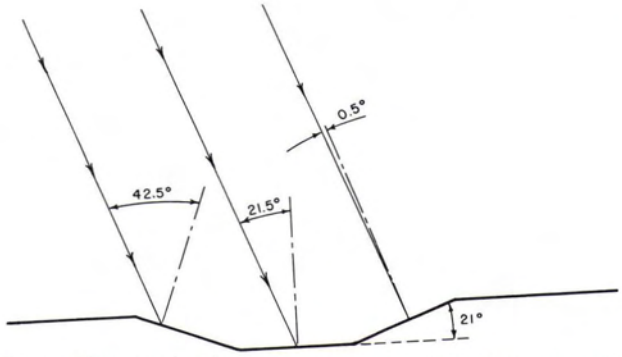

FIG. 2. Diagram showing cross-section of a fault-controlled gully and an incident signal with nominal incidence angle of 21.5° (Data Take AM82.2). Gully configuration produces local incidence angle of 0.5°.

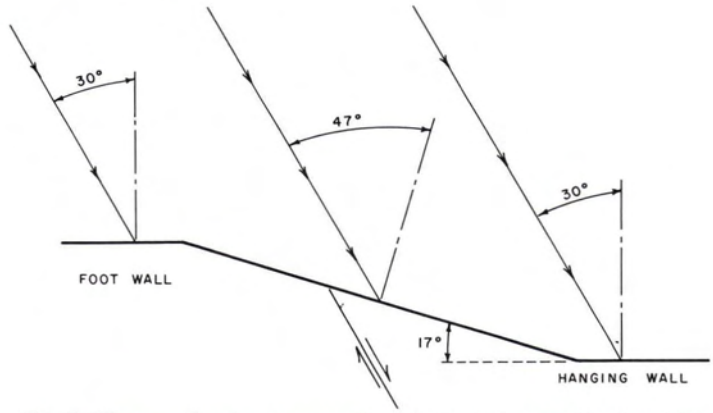

FIG. 3. Diagram showing cross-section of a typical normal fault and the resulting topography in Quaternary alluvium. With the footwall toward the near range and a 30° incidence angle (Data Take AL87.4), the local incidence angle on the fault scarp increases to 47°.

imagery, the areas of multiple coverage were severely reduced by the narrow swath width. In spite of this situation, stereo SIR-B image interpretation for the Candelaria site was attempted with Data Takes AM82.2 and AM66.2. Even though the look direction was the same, the different incidence angles (21.5° for AM82.2 and 40° for AM66.2) produced such differences in layover and foreshortening that stereo analysis was not feasible.

Garfield Hills/Pilot Mountains Test Site

The Garfield Hills, in eastern Mineral County, Nevada (Figure 1), expose a complexly deformed assemblage of allochthonous sedimentary and volcanic rocks and undeformed intrusive and extrusive rocks. Previous studies have demonstrated the presence of lithologically and structurally discrete tectonic units within the Garfield Hills (Oldow, 1976). The entire Garfield Hills were imaged by Data Take AL87.4.

Although the proposed continuation of the Excelsior fault zone (Stewart, 1985) is expressed as a negative topographic feature, many dip-slip faults will have a positive topographic expression. In order to determine the amount of fault-induced topographic variation discernible by the SIR-B system, two mapped dip-slip faults were examined on SIR-B imagery and in the field. One fault (fault A, Figure 1) bounds the eastern side of Garfield Flat with the up-thrown block toward the near range. The other fault (fault B, Figure 1) is on the western edge of the Pilot Mountains and the down-thrown block is toward the near range.

The feature on the east side of Garfield Flat is a continuation of a fault that juxtaposes Quaternary alluvium against bedrock and has been mapped and described by Dohrenwend (1982) as a fault-related lineament in Quaternary surficial deposits. The lineament in the Quaternary deposits is a slightly weathered scarp in the alluvial fan that slopes toward Garfield Flat. The scarp trends in a direction approximately sub-parallel to the azimuth direction of the SIR-B system (336°) and is 5 metres in height. Most of the alluvial fan is covered with gravelly soil, grass, and sagebrush. Examination of Data Take AL87.4 shows a faint, dark lineament at the location of the fault-related lineament (Plate 5). This feature was still difficult to detect after contrast enhancement and filtering procedures. The problem of detection is mainly a result of speckle and the fact that the fault-related lineament has the up-thrown block toward the near range, giving a dark lineament. The scarp slopes at 17° toward the far range and is within an area of reduced signal return caused by a local incidence angle of 47° (Figure 3). If the fault plane were dipping toward the near range, with the up-thrown block facing toward the far range, the 5-metre scarp would be far more obvious on the image.

Several faults in the alluvial fan of the Pilot Mountains have been mapped as late Cenozoic and described by Dohrenwend (1982) as faults forming fault scarps in early Quaternary, Tertiary alluvium, and latest Tertiary volcanic rocks. Lineaments are displayed as contrasting brightness, with the greater signal return corresponding to rougher areas that are higher on the alluvial fan and smoother areas of lesser signal return on the lower part of the alluvial fan. Field examination revealed that the greater amount of radar backscatter is a result of two erosional processes. First, because the down-thrown block faces toward the basin, erosion has been reactivated on the upper fan and has removed most of the silt-, sand-, and smaller cobble-sized sediment. This process has produced a rougher surface, with an average clast size of approximately 20 centimetres. Second, renewed erosion has cut small, closely spaced gullies of approximately one metre in depth into the upper part of the alluvial fan, producing rolling, hummocky topography. In this situation, some of the slopes are so oriented that the local angle of incidence is very small, and a large portion of the signal is returned to the antenna. Although there is a marked contrast between the surface roughness on either side of the fault, the corresponding differences in brightness on the imagery are subtle.

The Garfield Flat and Pilot Mountains sites provide two examples of how recent Basin and Range faulting can be expressed in radar images. Some faults may be so young, as the Garfield Flat example, that both the hanging wall and the foot wall are still within the smooth criterion for L-band wavelengths. If the up-thrown block faces toward the near range, detection will be even more difficult because of the greater local incidence angle on the fault scarp. The five-metre scarp, which is a very obvious feature in the field, is essentially at the threshold of detectability with SIR-B data. This problem can probably be overcome where multi-incidence angle SIR-B data is available.

The fault at the Pilot Mountains site, with up-thrown blocks facing toward the far range, is more apparent because the fault appears to be older, allowing greater time for erosional processes to produce a surface with detectable, contrasting roughness. These fault scarp features cannot be overlooked in the field, which suggests that greater SAR signal-to-noise ratios and/or ancillary data sets are necessary to detect unmapped faults.

SUMMARY

In spite of the variations in soil moisture and the different plant communities present, SIR-B data could not be used to detect these types of variations. Although soil moisture ranged from 1 percent to 15 percent, these variations could not be detected because the surface roughness varied independently of soil moisture. Morphological similarity of the vegetation and radar speckle were the major factors in the failure to detect differences in community structure.

The ability to identify negative topographic features produced by strike-slip faulting with SIR-B data is largely controlled by the

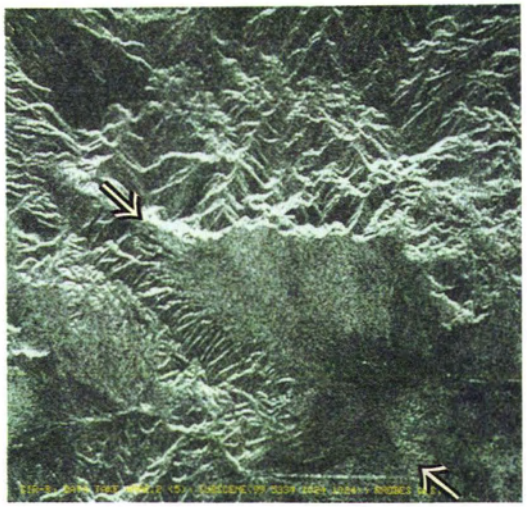

PLATE 1. SIR-B Data Take AM82.2, Candelaria site. Arrows point to a lineament coincident with the extension of the Excelsior fault.

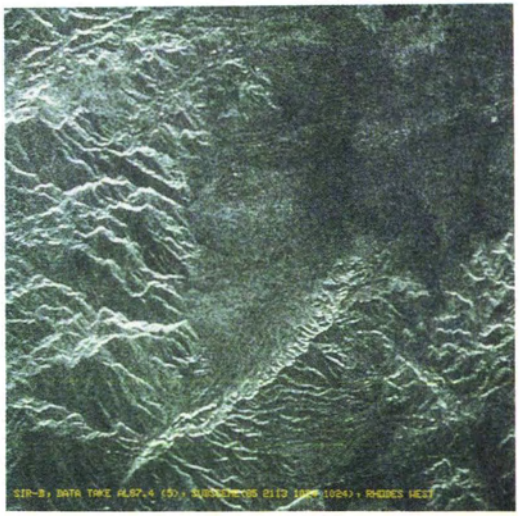

PLATE 2. SIR-B Data Take AL87.4, Candelaria site. Same area as Plate 1 but the Excelsior lineament is not visible because of unfavorable look direction.

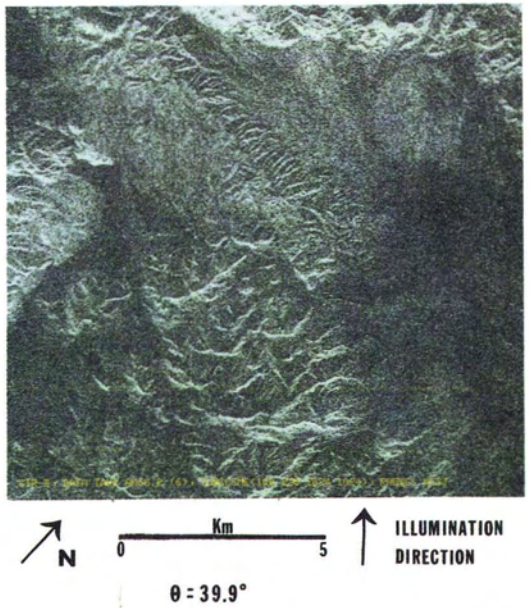

PLATE 3. SIR-B Data Take AM66.2, Candelaria site. Even though the look direction is optimum, the Excelsior lineament cannot be seen because of the large SIR-B incidence angle.

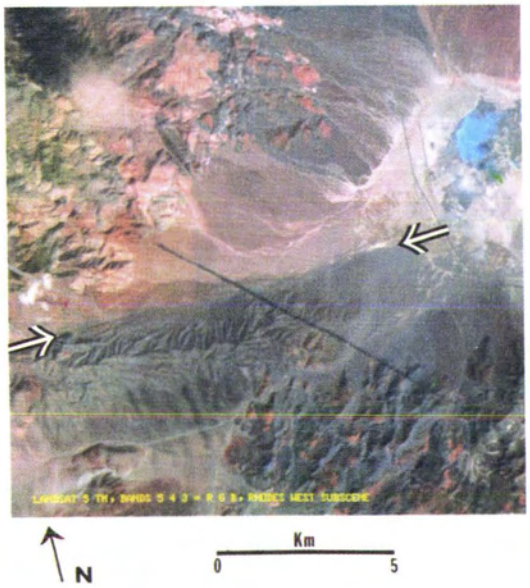

PLATE 4. Landsat 5 TM, Candelaria site. Bands 5, 4, and 3 are color-encoded red, green, and blue, respectively, Arrows point to a tonal lineament produced by boulders of differing lithology.

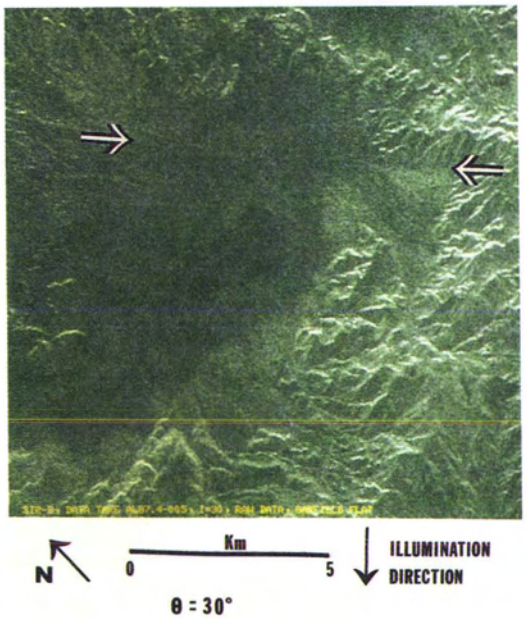

PLATE 5. SIR-B Data Take AL87.4, Garfield site. Arrows point to a lineament that is coincident with a fault scarp in Quaternary surficial deposits.

incidence angle. SIR-B data takes with small incidence angles will adequately display these types of features, although no new geological features of structural importance were recognized. Look direction is critical for identifying dip-slip faults in Quaternary sediments. Fault scarps are more readily identified when the hanging wall faces toward the near range; fault scarps several metres in height are very difficult to identify if the hanging wall faces toward the far range. A major hindering factor was the low signal-to-noise ratio of the SIR-B data. On many of the relatively higher quality SIR-B scenes there are very subtle suggestions of the presence of unmapped structural features. These features are very difficult to confirm in the field and, therefore, it is difficult to determine their geological validity. However, in many cases they are coincident with lineaments on Landsat TM imagery, and a number of them trend parallel to major structural features. The next phase of the investigation will involve the utilization of digital geophysical data to determine if these very subtle features on SIR-B imagery have significance with respect to structural geology and regional tectonics.

ACKNOWLEDGMENTS

This work was supported by the National Aeronautics and Space Administration under contract RAI No. LC-61130. Special thanks to JoBea Cimino, Charles Elachi, Annie Richardson, and Martin Ruzek for assistance.

REFERENCES

Billings, W.D., 1949. The shadscale vegetation zone of Nevada and eastern California in relation to climate and soils. *Amer. Midl. Nat.* 42: 87–109.

Brady, N.C., 1974. *The Nature and Properties of Soils*: 8th ed. Macmillan.

Bush, F.T., and F.T. Ulaby, 1978. An evaluation of radar as a crop classifier. *Rem. Sens. Environ.*, 7, p. 15–36.

Dohrenwend, J.C., 1982. *Map Showing Late Cenozoic Faults in the Walker Lake 1° × 2° Quadrangle*, Nevada-California. U.S. Geol. Survey, Map MF-1382-D.

Fowler, D., and D. Koch, 1982. The Great Basin, *Reference Handbook on the Deserts of North America* (Gordon Bender, ed.), Greenwood Press, Westport, Conn, 594 p.

Huete, A.R., D.F. Post, and R.D. Jackson, 1983. Soil spectral effects on 4-space vegetation discrimination. *University of Arizona Remote Sensing Newsletter*, 83–1.

Morain, S.A., and D.S. Simonett, 1966. K-band radar in vegetation mapping. *Photogrammetric Engineering*, 33, 730–740.

Munz, P.A., 1959. *A California Flora* (5th printing, 1970). Univ. of Calif. Press, Berkeley, 1681 p.

Oldow, J.S., 1976. Structural juxtaposition of allochthonous Triassic facies, Garfield Hills, western Navada. *Geol. Soc. America Abs. with Programs.* 8: 401.

Simonett, D.S. (ed.) 1983. *Manual of Remote Sensing*, 1 (2nd edition). Amer. Soc. of Photogrammetry, 1232 p.

Stewart, J.H., 1985. East-trending dextral faults in the western Great Basin: An explanation for anomalous trends of pre-Cenozoic strata and Cenozoic faults. *Tectonics*. 4: 547–564.

Ulaby, F.T., and P.P. Batlivala, 1976. Optimum radar parameters for mapping soil moisture. *IEEE Trans. on Geosci. Electronics*, GE-4:2, 81–93.

Wardley, N.W., E.J. Milton, and C.T. Hill, 1987. Remote sensing of structurally complex semi-natural vegetation - an example from heathland. *IJRS* 8(1): 31–43.

(Received 16 January 1987; revised and accepted 13 October 1987)